Preoperative Computed Tomography Imaging of the Sphenoid Sinus: Striving Towards Safe Transsphenoidal Surgery

John Raseman[1] Melike Guryildirim[2] André Beer-Furlan[3] Miral Jhaveri[2] Bobby A. Tajudeen[4] Richard W. Byrne[3] Pete S. Batra[4]

[1] Department of Diagnostic Radiology, Mallinckrodt Institute of Radiology, St. Louis, Missouri, United States
[2] Department of Diagnostic Radiology, Rush University Medical Center, Chicago, Illinois, United States
[3] Department of Neurological Surgery, Rush University Medical Center, Chicago, Illinois, United States
[4] Department of Otorhinolaryngology–Head and Neck Surgery, Rush University Medical Center, Chicago, Illinois, United States

Address for correspondence John Raseman, MD, Department of Diagnostic Radiology, Mallinckrodt Institute of Radiology, 216 South, Kingshighway Boulevard, St. Louis, MO 63110, United States (e-mail: jraseman@wustl.edu).

J Neurol Surg B 2020;81:251–262.

Abstract

Introduction Preoperative high-resolution computed tomography (HRCT) is essential in patients undergoing transsphenoidal surgery to identify potential high-risk anatomic variations. There is no consensus in the literature, as to which grading system to use to describe these variants, leading to inconsistent terminology between studies. In addition, substantial variability exists in the reported incidence of anatomic variants. In this study, we performed an institutional imaging analysis and literature review with the objective of consolidating and clearly defining these sphenoid sinus anatomical variations. In addition, we highlighted their surgical implications and propose a checklist for a systematic assessment of the sphenoid sinus on preoperative CT.

Methods Review of the literature and retrospective analysis assessing several imaging parameters in 81 patients who underwent preoperative HRCT imaging for endoscopic transsphenoidal tumor resection from January 2008 through July 2015 at Rush University Medical Center.

Results The most common sphenoid pneumatization patterns were sellar (45%) and postsellar (49%) types. Anterior clinoid process (ACP) pneumatization was seen in 17% of patients with high concordance of ipsilateral optic nerve (ON) protrusion. ON protrusion and dehiscence was present in 17 and 6% of patients, respectively. Internal carotid artery (ICA) protrusion and dehiscence was present in 30 and 5% of patients, respectively. Dehiscence rates from local bone invasion overlying the ICA and ON occurred in 17 and 4% of cases, respectively.

Conclusions Our study highlights and reviews the key variants that have potential to impact surgical complications and outcomes in a heterogeneous patient population. The proposed preoperative CT checklist for patients, undergoing transsphenoidal surgery, consistently identifies these higher risk anatomical variants.

Keywords
- radiology
- transsphenoidal surgery
- sphenoid sinus
- anatomic variation
- computed tomography
- preoperative Imaging

received
October 24, 2018
accepted after revision
April 4, 2019
published online
May 28, 2019

DOI https://doi.org/10.1055/s-0039-1691831.
ISSN 2193-6331.

Introduction

The transsphenoidal approach for sellar tumor resection has been the standard of care for decades, as it provides a safe and direct route to the ventral skull base.[1] The sphenoid bone is one of the most complex bones in the human body and is made up of four parts: the body, the lesser and greater wings, and the pterygoid processes.[2] The sphenoid sinus is a part of the sphenoid body and it is considered the main surgical entry point to the ventral skull base due to its location and bony anatomical landmarks. The appearance of the sinus depends largely on its degree of pneumatization.[3,4]

Preoperative imaging assessment is essential to optimal surgical planning. The evaluation of the sphenoid sinus should include the pathological displacement of the normal anatomy by the tumor or anatomical variations that can put patients at risk for complications during transsphenoidal surgery. The rates of protrusion, dehiscence, and pneumatization reported in prior studies are variable (►**Tables 1** and **2**). The variability may not only relate to the differences in patient populations, but also, how these terms are defined and measured.

In this study, we performed an institutional imaging analysis and literature review with the objective of consolidating and refining these sphenoid sinus anatomical variations. In addition, we highlighted their surgical implications and propose a checklist for systematic assessment of the sphenoid sinus on preoperative computed tomography (CT).

Methods

A retrospective review of patients, who underwent preoperative CT imaging ($\leq$1 mm axial acquisitions with 1 mm multiplanar reformatted images) for endoscopic transsphenoidal tumor resection from January 2008 through July 2015 at Rush University Medical Center, was performed. The relevant clinical information including patient's demographics (age, sex, and ethnicity) and history, tumor type, operative parameters, and follow-up data was obtained. Patients with preoperative CT imaging with $>$ 1 mm slice thickness were excluded from the analysis.

Imaging analysis was resultant of a consensus between the simultaneous assessments of a senior radiology resident and a neuroradiology fellow. Any indeterminate cases were resolved by a neuroradiology attending with 20 years of experience.

The pneumatization of the sphenoid sinus, lateral recess, anterior clinoid process (ACP), and dorsum sellae was evaluated. The CT scans were also assessed for sphenoethmoidal (Onodi) cells, sphenoid osteology, septation pattern/insertion site, protrusion, and/or dehiscence of the internal carotid artery (ICA) and optic nerve (ON).

The detailed methods used for imaging analysis were as follows:

- *Sphenoid sinus pneumatization:*

Sphenoid pneumatization (►**Fig. 1**) was modeled after the Güldner classification, which describes conchal, presellar, sellar, or postsellar types by evaluating the posterior extent of pneumatization with respect to the sella.[4] In the midline image, a plumb line is drawn perpendicular to the planum sphenoidale at the anterior and posterior walls of the sella and then compared with the posterior extent of pneumatization. The "conchal" pneumatization describes minimal or absent pneumatization. "Presellar" pneumatization describes the

Table 1 Incidences of sphenoid pneumatization patterns by classification system

Hammer's/Radberg's Classification				
Paper	**Conchal (%)**	**Presellar (%)**	**Sellar (%)**	
Current study, year	0	6	94	
Hamberger et al,1961[5]	3	11	86	
Renn et al, 1975[6]	0	20	80	
Fujii et al, 1979[7]	0	24	76	
Banna and Olutola, 1983[8]	3	11	86	
Ouaknine and Hardy, 1987[9]	3	12	85	
Sethi and Pillay, 1995[10]	0	27	73	
Sareen et al, 2005[11]	–	25	75	
Abuzayed et al, 2009[12]	–	20	80	
Lazaridis et al, 2010[13]	4	28	68	
Wang et al, 2010[14]	0	2	98	
Lu et al, 2011[15]	6	29	66	
Perondi et al, 2013[16]	5	9	86	
Vaezi et al, 2015[17]	2	24	74	
Anusha et al, 2014[18]	$<$ 1	7	93	
Locatelli 2017[19]	1	5	94	
Güldner's Classification				
Paper	**Conchal (%)**	**Presellar (%)**	**Sellar (%)**	**Postsellar (%)**
Current study, year	0	6	45	49
Liao et al, 2001[20]	4	36	14	46
Kayalioglu et al, 2005[21]	2	9	53	36
Zhou 2005[22]	3	26	59	12
Hamid et al, 2008[23]	2	21	55	22
Cho et al, 2010[24]	1	9	47	43
Li et al, 2010[25]	2	31	21	47
Güldner et al, 2012[4]	$<$ 1	7	57	36
Tomovic et al, 2013[26]	2	7	48	43
Wiebracht and Zimmer, 2014[27]	0	9	37	54
Halawi et al, 2015[28]	0	20	51	29
Rahmati et al, 2016[29]	0	2	15	84

Table 2 Rates of neurovascular protrusion[a]/dehiscence secondary to anatomic variation

Paper (study, year)	Sample type/size	Protrusion ON (%)	Dehiscence ON (%)	Protrusion ICA (%)	Dehiscence ICA (%)
Renn 1975[6]	Cadaver, 50	–	4	–	4
Fujii et al, 1979[7]	Cadaver, 25	–	4	–	8
Cho et al, 2010[24]	Cadaver, 59	56	4	34	2
Meloni et al, 1992[30]	CT, 100	–	8	–	5
Dessi et al, 1994[31]	CT, 150	8	–	–	–
DeLano et al, 1996[32]	CT, 150	–	24	–	–
Sirikci et al, 2000[33]	CT, 92	32	23	26	23
Sapçi et al, 2004[34]	CT, 100	–	14	–	–
Kazkayasi et al, 2005[35]	CT, 267	4	1	5	2
Unal et al, 2006[36]	CT, 56	31	8	30	5
Hewaidi and Omami, 2008[37]	CT, 300	35	30	41	30
Davoodi et al, 2009[38]	CT, 399	26	37	42	42
Güldner et al, 2012[4]	CBCT, 644	14	17	11	3
Rahmati et al, 2016[29]	CBCT, 103	33	–	39	–
Batra et al, 2004[39]	HRCT, 64	–	–	16	13
Tomovic et al, 2013[26]	HRCT, 170	26	2	28	3
Anusha et al, 2014[18]	HRCT, 300	2	7	3	10
Itagi et al, 2017[40]	HRCT, 100	25	18	–	
Dal Secchi et al, 2018[41]	HRCT, 90	–	–	54	4
Current Study	HRCT, 81	17	6	30	5

Abbreviations: CT, computed tomography; HRCT, high-resolution CT; ICA, internal carotid artery; ON, optic nerve.
[a]Some of the above papers were re-calculated using 50% exposure or analogous definition of protrusion.

posterior extent of pneumatization anterior to the anterior wall of the sella. "Sellar" pneumatization extends posterior to the anterior wall of the sella but not beyond the posterior wall. "Postsellar" pneumatization extends beyond the posterior wall of the sella. An additional postsellar subdivision in the Güldner classification was not utilized as dorsum sella pneumatization was evaluated separately, in our study.

- *Lateral recess pneumatization:*

Lateral recess pneumatization (►**Fig. 2**) was defined as pneumatization extending up to or beyond a line drawn between the maxillary and vidian nerves (corresponding to Vaezi's type II/III).[17]

- *Anterior clinoid process (ACP) pneumatization:*

It is pneumatization extending into the body of the ACP beyond the level of the optic strut (►**Fig. 3**).

- *Dorsum sellae pneumatization:*

It is defined as pneumatization extending into the superior aspect of the dorsum sellae (►**Fig. 4**).

- *Sphenoethmoid cells (Onodi cells):*

It is extension of the most posterior ethmoid air cell superolaterally to the sphenoid sinus extending adjacent to the ON (►**Fig. 5**).

- *Sphenoid osteology (access dimensions):*

Multiple measurements of the sphenoid sinus were performed (►**Fig. 6**) including presellar height, presellar depth, maximum infrasellar depth, presellar width, maximum sphenoid sinus width, and intercarotid distance at the level of the midcavernous ICA segment.[27] Intercarotid distance measurements were obtained at a midcavernous ICA level where there was generally greatest protrusion into the sphenoid sinus.[23,27] The intercarotid distance was measured at the same level in patients with bony destruction by a mass.

- *Septation pattern/insertion site:*

Sphenoid septa were defined as single or multiple. The category of multiple septa included diverging, accessory, double, cruciate, etc.[11,23,26,27,42,43] Each septum was evaluated individually to determine whether it is inserted on the bone underlying the ON, ICA, both, or neither (►**Fig. 7**).

- *Protrusion and/or dehiscence of the ICA and ON:*

Protrusion of a neurovascular structure into the sphenoid sinus was defined as whether ≥50% of a structure was displaced into the sphenoid sinus (►**Fig. 8**). To determine the percentage of neurovascular protrusion, a line was drawn

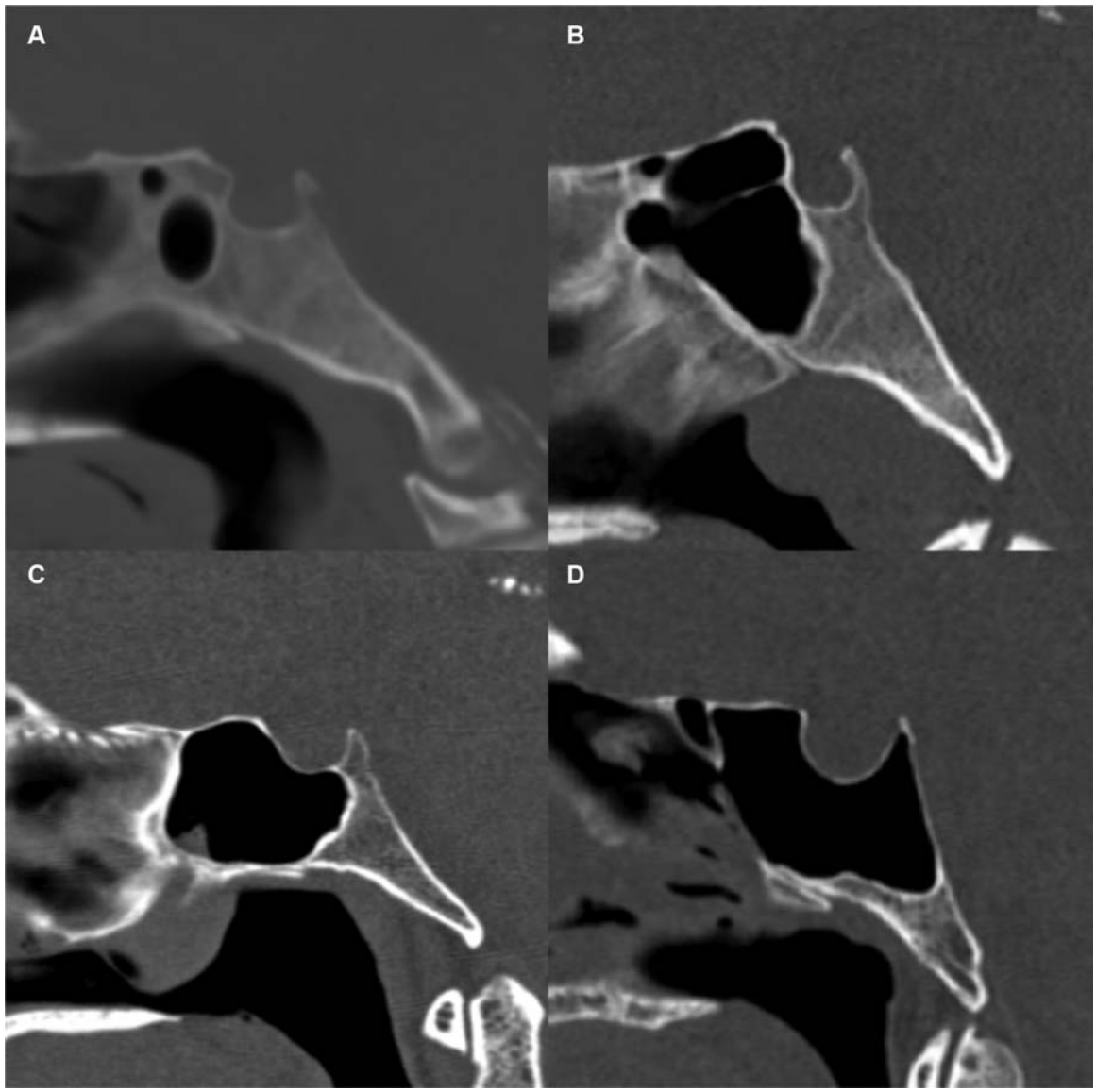

Fig. 1 Güldner's classification of sphenoid sinus pneumatization. Sagittal CT images in the midline demonstrate examples of (**A**) conchal, (**B**) presellar, (**C**) sellar, and (**D**) postsellar pneumatization types. Note that the presellar pneumatization example (**B**) is on the margin of pre-sellar and sellar types, but is ultimately presellar as only the rostrum of the sella is exposed and there is no pneumatization along the floor of the sella. CT, computed tomography.

between the outer margins of the bony indentation and then the percentage of the neurovascular structure encompassed by that line was evaluated. ICA and ON protrusion was evaluated on axial and coronal images, respectively. Dehiscence of neurovascular structures was defined as absence of bone or inability to discern the presence of bone overlying the ICA or ON with attempted confirmation on multiples slices and/or planes (►**Figs. 9** and **10**). Cases, in which the walls of the optic canal or carotid sulci were absent, secondary to mass invasion were considered "dehiscent by mass" (►**Fig. 11**).

- *Variation due to pathology or previous surgery:*

Anatomic variability due to the existing tumor, secondary pathology, prior functional endoscopic sinus surgery (FESS), or congenital etiologies was noted.

Review of the literature was performed using PubMed search filters: "Sphenoid Sinus,"[Mesh] AND "Surgical Procedures, Operative,"[Mesh] AND "pneumatization"[All Fields]. Additional relevant articles were obtained by reviewing the references of the articles retrieved from the primary search.

Results

Demographics

Our cohort comprised in 81 patients, 44 (54%) males and 37 (46%) females. The mean age was 53.7 years with patient ages ranging from 17 to 83 years. The racial makeup of patients was 65, 16, 14, and 4% White, Black, Hispanic, and Asian, respectively.

The most common diagnosis was pituitary adenoma (85%), followed by Rathke's cleft cyst (5%). Additional tumor types included meningioma, pilocytic astrocytoma, schwannoma,

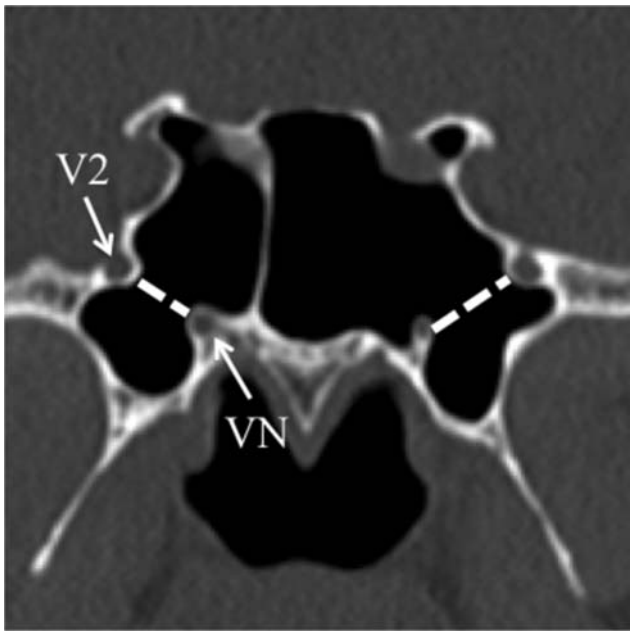

Fig. 2 Lateral recess pneumatization. Coronal CT image demonstrates bilateral pneumatization of the lateral recesses with air extending beyond a line (dashed line) between to the maxillary nerve (V2) and vidian nerve (VN), which was modeled after Vaezi's type II/III (Vaezi et al[17]).

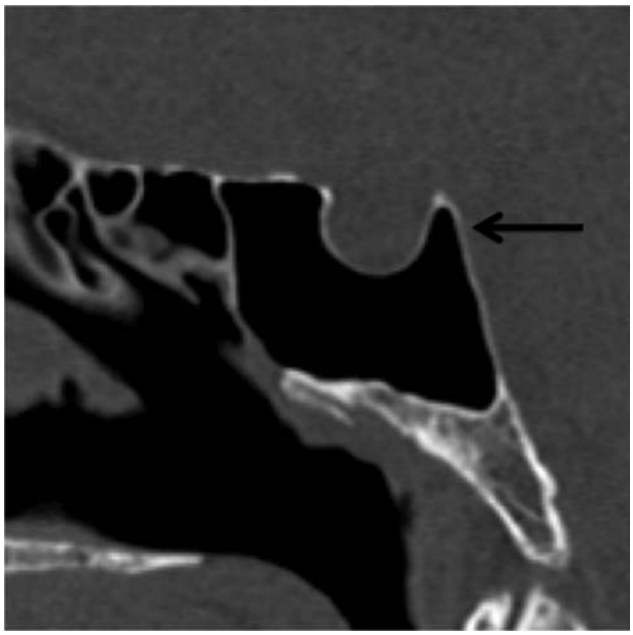

Fig. 4 Dorsum sella pneumatization. Sagittal CT demonstrates pneumatization extending into the dorsum sella (black arrow). CT, computed tomography.

pituitary xanthogranuloma, metastatic breast cancer, cholesterol granuloma, osteosarcoma, and pituitary hyperplasia.

CT Analysis

The most common sphenoid pneumatization patterns in our study were sellar (53%) and postsellar (42%) types. The conchal pneumatization pattern was not seen in any of our patients. Only 5% of patients had a presellar pneumatization pattern. Two patients had marked invasion of the sphenoid sinus precluding identification of their pneumatization pattern and were excluded from this analysis.

ACP pneumatization was seen in 19% of patients. Of 24 total instances of ACP (by side), 18 were demonstrated ipsilateral protrusion of the ON. Only a single case of ON protrusion was present without ipsilateral clinoid process pneumatization.

Dorsum sellar pneumatization pattern was seen in 5% of patients. One or more sphenoethmoid cell was present in 12% of patients.

The presellar height measured 24 mm (14–31 mm). The presellar depth of 13 mm (2–20 mm) with a maximum infrasellar depth measured 25 mm (2–39 mm). The presellar width

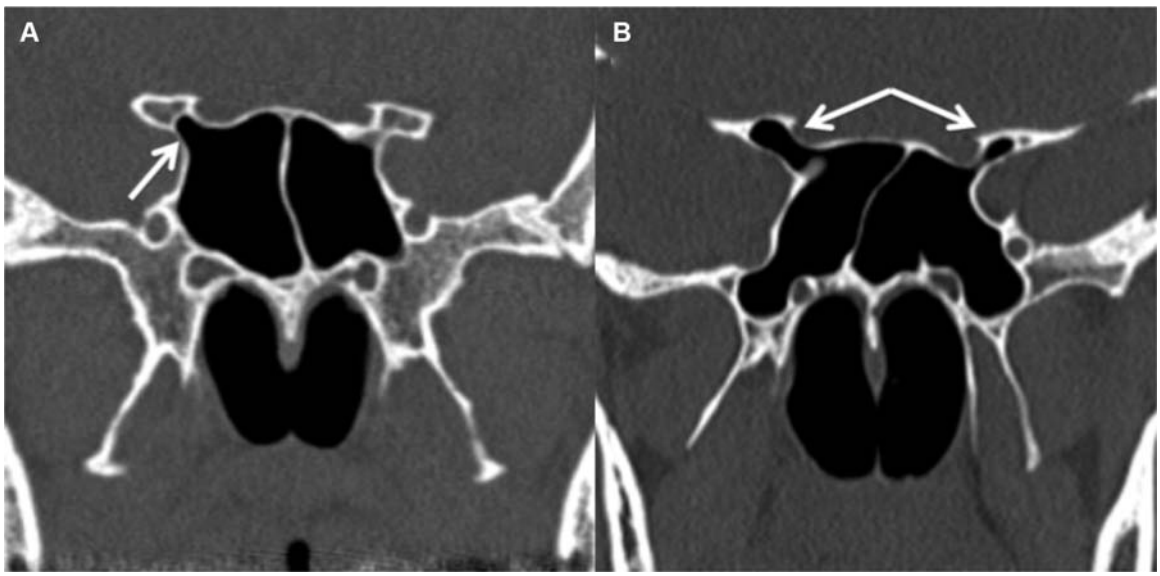

Fig. 3 Anterior clinoid process (ACP) pneumatization. Coronal CT image (**A**) demonstrates pneumatization of the right optic strut (white arrow), which does not extend into the ACP. Second coronal CT image (**B**) demonstrates pneumatization of the optic strut and portions of the bilateral ACPs, right greater than left (white arrows). CT, computed tomography.

Fig. 5 Sphenoethmoid cell (Onodi cell). Coronal CT image demonstrating right sided sphenoethmoid cell (Onodi cell) (white arrow) abutting the adjacent optic nerve/canal (black arrow). CT, computed tomography.

measured 16 mm (10–33 mm) with a maximal sphenoid width of 36 mm (21–67 mm). The intercarotid distance measured 18 mm (9–26 mm) at the level of the mid-cavernous segment.

Lateral recess pneumatization was present on at least one side in 59% of patients.

A majority of patients had multiple sphenoid septa (57%). Approximately 60% of patients had a septum inserting on either the ON, ICA, or both. A majority of patients (64%) with lateral recess pneumatization demonstrated an accessory septum along the posterolateral margin of the sinus at the origin of the lateral recess; often originating along the carotid sulcus. A majority of patients (72%) with this type of accessory septa had lateral recess pneumatization.

Protrusion of the ICA into the sphenoid sinus was present in 30% of cases. Dehiscence of the ICA secondary to anatomic variation occurred in 5% of all cases. One of four cases of ICA dehiscence secondary to anatomic variation had concomitant protrusion.

Protrusion of the ON into the sphenoid sinus was present in 17% of cases. Dehiscence of the ON, secondary to anatomic variation, occurred in 6% of all cases. Three of five cases of ON dehiscence secondary to anatomic variation had concomitant protrusion.

A minority of patients had invasion of the sphenoid sinus making it difficult or impossible to evaluate portions of the sinus. Approximately 6% of patients had invasion preventing evaluation of sphenoid dimensions. Only 2% of patients had such extensive obliteration of the sinus that the sellar pneumatization pattern could not be evaluated. Destruction of the bone, overlying the ICA or ON, ("dehiscence by mass") was presented in 17 and 5% of patients, respectively. Nine percent of patients had evidence of prior functional endoscopic sinus surgery.

Discussion

Literature Review and Surgical Implications

Demographics and Tumor Types

Demographics of our patient population mirrored that of the United States as a whole.[44] Our patient pool was comprised predominantly of patients with benign tumors, the vast majority of which were pituitary adenomas. Several these adenomas were demonstrated invasion of surrounding contiguous structures including the cavernous and sphenoid sinuses putting these patients at higher risk of vascular injury at resection. Many of the prior studies were intended to evaluate normal anatomy and, therefore, would have excluded patients in our study.[17,26,27,34,38] Our intention was to specifically evaluate a representative patient population undergoing transsphenoidal surgery.

Sphenoid Pneumatization

There is high variability in the rates of sphenoid pneumatization, which are summarized in ►**Table 1**. Similar to prior

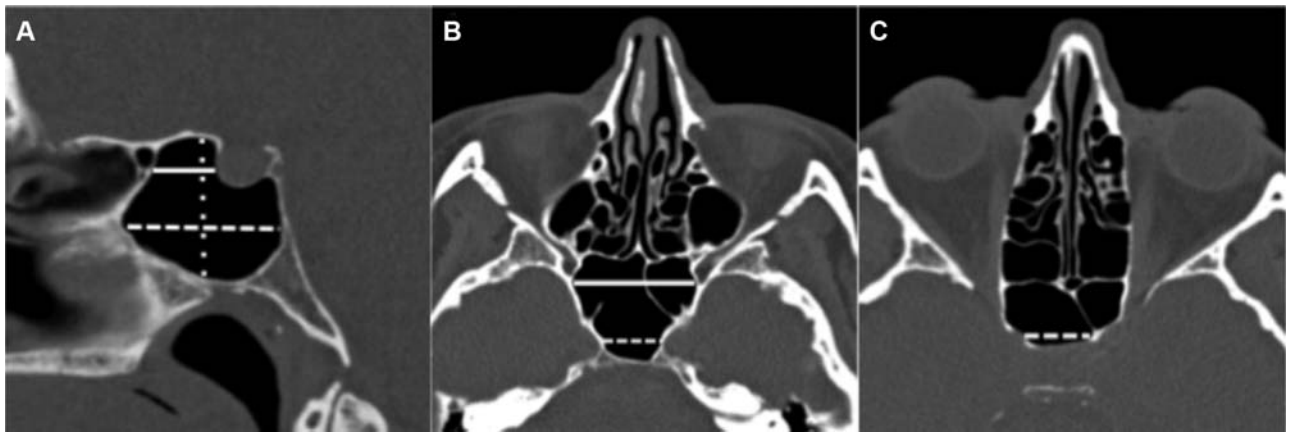

Fig. 6 Sphenoid osteology. Sagittal midline CT image (**A**) demonstrates presellar depth (solid line), infrasellar depth (dashed line), and presellar height (dotted line). Both measurements are drawn parallel to the planum sphenoidale/ethmoidale. Axial CT image (**B**) demonstrates intercarotid distance (dashed line) and sphenoid width (solid line). Axial CT image (**C**) demonstrates sellar width (dashed line). Measurements were adapted from Wiebracht and Zimmer[27]. CT, computed tomography.

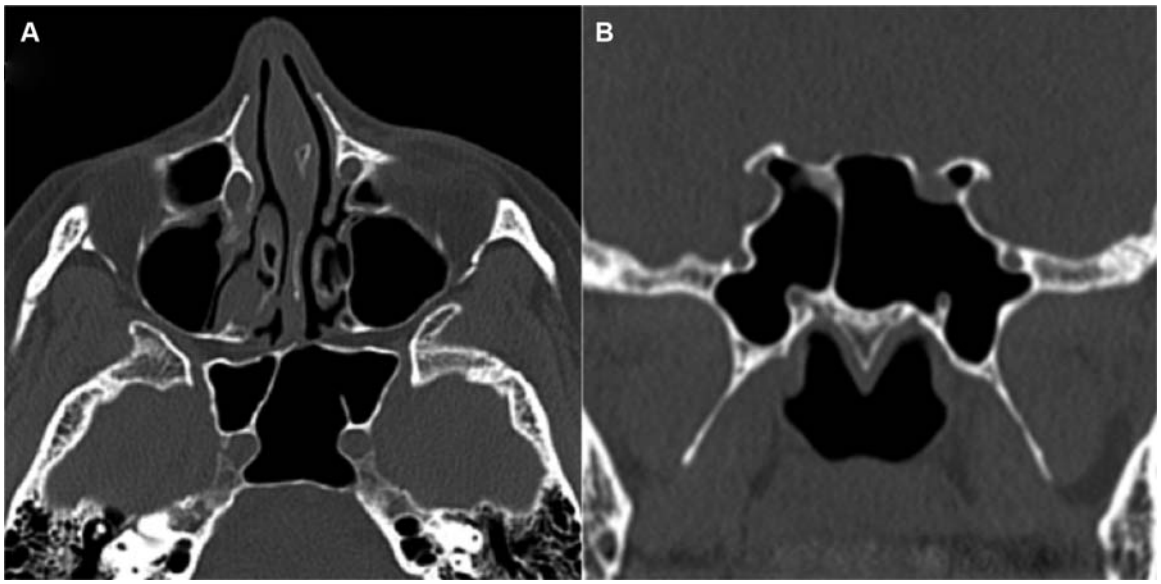

Fig. 7 Septation pattern. Axial CT image (**A**) demonstrates insertion of the sphenoid septum on a protruding right ICA with an accessory septum on a protruding left ICA. Coronal CT image (**B**) demonstrates sphenoid septal inserting over the right optic nerve. Possible dehiscence of the left ON was questioned; however, this was felt to relate to partial volume averaging effects given thin bony coverage was seen on additional reformatted images. CT, computed tomography; ICA, internal carotid artery; ON, optic nerve.

studies, the majority of our patients demonstrated sellar and postsellar pneumatization types, though several studies had a higher proportion of presellar pneumatization compared with this study. Anatomic variability is the major factor in reported variability between patients; however, there are likely study design differences that contribute to differences in reported incidences. First, comparing the incidence of sellar and postsellar pneumatization to prior studies was confounded by older studies using the Radberg classification and the majority of more recent studies using the Güldner classification.[3,4] Next, defining pneumatization accurately can be subject to interobserver variability when pneumatization is at the margins of the anterior or posterior sella (►**Fig. 1B**). Last of all, differences in methodology between cadaveric, CT, and radiographic studies make comparison difficult. For example, our patient population did not include a case of conchal pneumatization, similar to several other papers. Articles commonly cite a study by Tan and Ong as having a conchal pneumatization rate of 28% in their cadaveric cohort.[43] However, the patients were analyzed by side and not in the midline. In their paper, they do not report a single case of bilateral conchal pneumatization, just as in our study. The paper in our review with the next highest incidence of conchal pneumatization was 6%.[15]

Identification of presellar and conchal pneumatization types is important as they provide the greatest obstacle to accessing the sella. The main bony surface landmarks, such as the sellar rostrum/floor, parasellar cavernous ICA bend, lateral optic–carotid recess, and clival recess are not present. Previously, these types of pneumatization were considered as a relative contraindication to transsphenoidal surgery. Nowadays, the better visualization with endoscopes, improved anatomical knowledge of the ventral skull base, and use of intraoperative navigation system facilitates safe sellar bone drilling and surgery.[19] Despite the use of navigation systems, the sellar drilling should always start at the midline where there is lesser chance of vascular injury. Once a bone opening is achieved and dura mater is exposed, its curvature and palpation of the inner skull base surface provides good intraoperative information on the anatomy of the sella and proximity to the cavernous sinus and ICA.

Lateral Recess Pneumatization

A binary classification was used in this study, defining pneumatization as present, if it extended up to or beyond a line drawn dissecting the maxillary and vidian nerves (corresponding to Vaezi's type II/III; ►**Fig. 2**).[17] The majority of our patients demonstrated lateral recess pneumatization on at least one side.

Pneumatization of the lateral recess results in increased exposure of the vidian and maxillary nerves and impacts access to endoscopic endonasal approaches to the middle cranial fossa, infratemporal fossa, and petrous apex/infrapetrous region. In general, these nerves may be exposed to undesirable injury when accessing the middle cranial fossa. On the other hand, identification and exposure of the vidian and/or maxillary nerves is needed when performing approaches to the infratemporal fossa and petrous apex/infrapetrous region. Lateral recess pneumatization facilitates and often shortens the time for this surgical step of the approach.

The lateral recess pneumatization is of secondary importance in patients undergoing transsphenoidal access to sellar pathologies.

ACP Pneumatization

ACP pneumatization is present in a minority of patients, 17% in our series and 6 to 29% in our literature review.[14,18,33,35–37,45–47] Like several other studies, our study found a high number of patients demonstrating ON protrusion when ipsilateral ACP was present.[18,31,33,35,40] Patients with pneumatization, only extending into the optic strut, generally did not meet the criteria

Fig. 8 Neurovascular protrusion. Neurovascular structures depicted as white shapes. Black dashed lines drawn between the outer margins of bony indentation on the sphenoid sinus resulting from the neurovascular structure. The degree of the neurovascular structure encompassed by the dashed line with respect to the sinus is then visually assessed. ICA protrusion was assessed on axial images and ON protrusion was assessed on coronal images. Axial CT image (**A**) demonstrates protrusion of bilateral ICAs with significantly greater than 50% of the ICAs protruding medially to the dashed line. Axial CT image (**B**) demonstrates approximately 50% of the right ICA and 40% of the left ICA medial to the dashed lines. The right ICA would, therefore, barely meet criteria for calling protrusion, whereas the left ICA would be below the threshold. Coronal CT image (**C**) demonstrates bilateral protrusion of the ONs, with greater than 50% of the ON lumen encompassed by the dashed lines. Coronal CT image (**D**) demonstrates slight indentation of the sphenoid sinus by the right ON without protrusion of either ON. The entirety of the ONs are beyond the dashed lines at the margin of the sinus. CT, computed tomography; ICA, internal carotid artery; ON, optic nerve.

for ON protrusion as commonly seen in patients with ACP pneumatization.

The lateral optic–carotid recess is the optic strut impression on the sphenoid sinus bony surface. The pneumatization of the optic strut and/or ACP facilitates the identification of the ONs, optic canal and parasellar cavernous ICA during transsphenoidal surgery.

Dorsum Sella Pneumatization

In our series, only a small minority (5%) of patients had dorsum sellar pneumatization compared with the 8 to 14% described in prior studies.[23,27] The presence of dorsum sellar pneumatization can predispose patients to posterior sellar and upper clivus bone injury and cerebrospinal fluid (CSF) leak.[23]

Sphenoethmoid Cells (Onodi Cells)

At least one sphenoethmoid cell was pneumatized in 12% of patients, similar to prior examinations (ranging from 5–15%).[24,26,30,34–36,43,48] This variant is most commonly associated with risk of ON injury at surgery as attempt is made to enter the sphenoid sinus through the posterior wall of the ethmoid.[49] Recognition of this variant is important to avoiding this unnecessary complication as removal of sphenoethmoidal air cells can be critical to obtaining a wide sellar access.[39] The

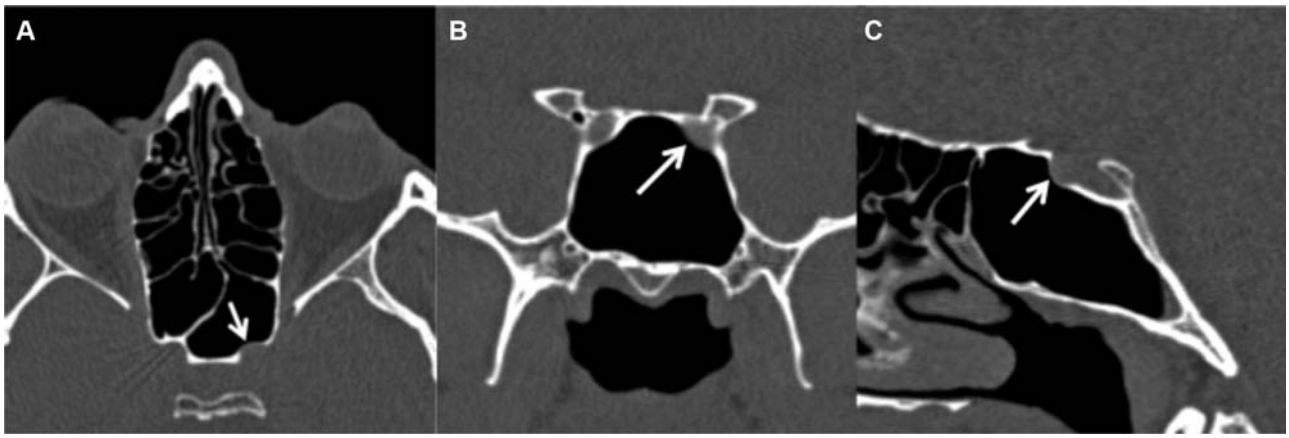

Fig. 9 Possible ICA dehiscence. Axial CT image (**A**) demonstrates possible left ICA dehiscence with minimal density along the anterior margin of the ICA (white arrow). Coronal CT image (**B**) of the same patient demonstrates more convincing dehiscence without any density along the margin of the ICA. However, sagittal CT image (**C**) demonstrates a possible thin rim of bony coverage of the margins of the ICA. This figure demonstrates the difficulty in confidently differentiating thin bony coverage from dehiscence. CT, computed tomography; ICA, internal carotid artery.

Fig. 10 ICA dehiscence. Axial CT image (**A**) and coronal image (**B**) demonstrate findings more confidently demonstrating right ICA dehiscence as compared with ►**Fig. 9**. CT, computed tomography; ICA, internal carotid artery.

ON is located at the apex of the cell and, therefore, the cell should be entered inferomedially instead of posterolaterally to avoid nerve injury[2] (►**Fig. 5**).

Sphenoid Osteology

The sphenoid osteology of our patients was similar to the paper by Wiebracht and Zimmer which studied patients undergoing neuronavigation for various intracranial pathologies.[27] Small sphenoid volumes are best evaluated subjectively or volumetrically as patients with expansile sellar lesions often still had large sphenoid dimensions with subjectively low pneumatized sinus volume related to mass expansion into the sphenoid. Volumetric analysis requires postprocessing and does not change clinical management and, therefore, subjective analysis of residual sphenoid size is felt to be appropriate in cases where masses encroach on or invade it.

The intercarotid distance in our patients was similar to prior with our average intercarotid distance measuring 18 mm, as compared with 15 to 23 mm in prior exams.[12,23,50] The highest intercarotid distances in our study were found in cases where tumors caused laterally displacement of the cavernous ICA. Narrowing of the intercarotid distance ("kissing carotid arteries") puts the carotids at potential risk for injury and individual analysis of the risks and benefits should be done when transsellar approach is required.

Septation Pattern and Insertion Site

In the vast majority of cases, the sphenoid sinus is divided by a dominant septum into smaller compartments of unequal sizes. These compartments can be further subdivided by additional septa which are commonly at the sites of former synchondroses.[51]

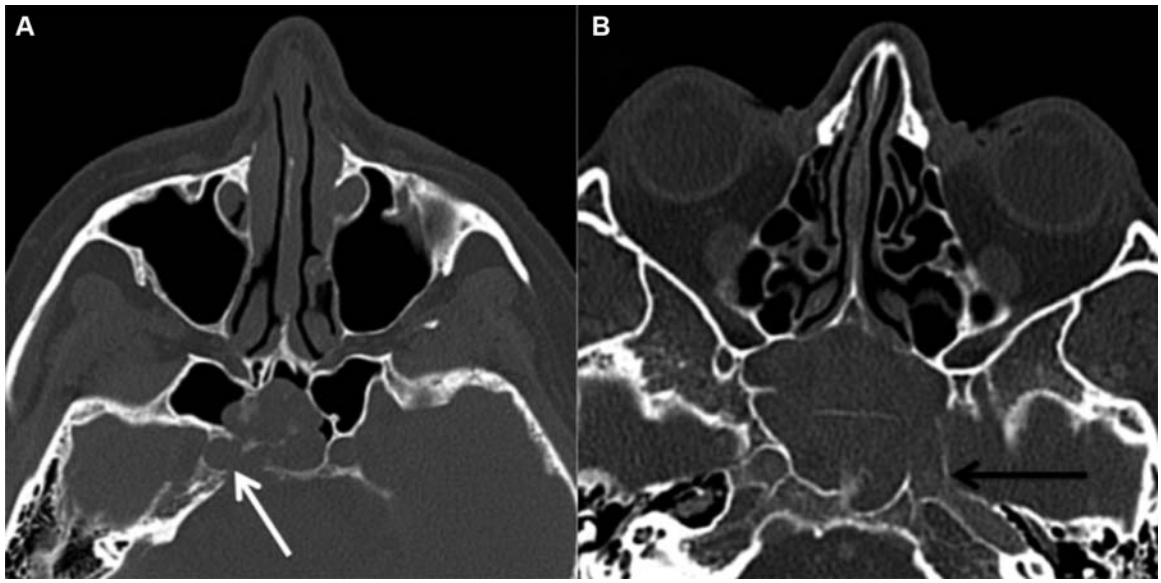

Fig. 11 ICA dehiscence by mass. Axial CT images (**A, B**) demonstrate right ICA dehiscence by mass invasion (white arrow) and left ICA dehiscence by mass invasion (black arrow) respectively. CT, computed tomography; ICA, internal carotid artery.

We defined septa, as single or multiple, given the variability in nomenclature for describing the presence of more than a single septum (examples include diverging, accessory, multiple, double, cruciate, etc.).[11,23,26,27,42,43] The majority of our patients had multiple septa (57%) and all of our patients had at least one septum, well, within ranges of prior studies (single, 20–77%; multiple, 20–80%). The majority of patients (60%) had a septal insertion over the ICA, ON, or both. This variant has been previously reported to be a source of potential injury risk to these structures with septal resection; however, their occurrence is exceedingly common and the incidence of injury to these structures are extremely low.[31] We still feel the practice of identifying insertion of septa on neurovascular structures is beneficial, especially in cases of overlying bony thinning, simply given the potentially catastrophic consequences of neurovascular injury.

Protrusion and/or Dehiscence of the ICA and ON

There is substantial variation of how the term "protrusion" is defined in the literature. We adopted the definition of protrusion as having greater than 50% exposure of the structure into the sinus[26,33,36] (►**Fig. 8**). Multiple studies defined protrusion as any degree of indentation of the structure into the sinus.[37,38] Such liberal definitions of protrusion may lessen the clinical importance of identifying this potentially higher risk anatomic variant, given that some degree of bulge is seen in most patients.[4,32,39] Analogous descriptors from prior studies, such as "free course" were not utilized. Multiple grading systems have been proposed to describe protrusion, which are not consistently used between studies and, therefore, create confusion in comparing their results.[4,32,34,39] We feel a cut-off of 50% is intuitive and simple to apply, though there will be some degree of interobserver variability.

Our study had respective protrusion rates for the ON and ICA of 17 and 30%, well within the range of prior examinations (►**Table 2**). Prior studies were only used as comparison when we could apply the definition of 50% neurovascular exposure or analogous description based on the data in their paper. Protrusion rates of the ICA were higher in patients with sellar and postsellar pneumatization types, though could not be statistically analyzed due to the small number of patients with presellar pneumatization in our cohort. A cadaveric study by Cho et al found higher rates of ON, ICA, vidian, and maxillary nerve protrusion with increasing pneumatization.[24]

A cadaveric study by Fujii et al found the bone overlying the ON and ICA is less than 0.5 mm in diameter in the majority of patients (78 and 88%, respectively) but dehiscent in a minority of cases (4 and 8%, respectively).[7] Early CT studies performed without high-resolution (HR) acquisitions may have been inaccurate for assessment of bony dehiscence. A 1996 study using 4 mm axial sections found an overall dehiscence rate of 24% dehiscence.[32] This paper found a dehiscence rate of 71% in patients with concurrent ON protrusion ($>$ 50%). In contrast, we found ON dehiscence in only 6% of patients secondary to anatomic variation with dehiscence in only 21% of cases of protrusion. The low dehiscence rate, we found, is supported the existing cadaveric studies and the majority of HRCT studies. However, despite the low observed dehiscence rate, our data does support their findings of increased potential for ON dehiscence in patients with concurrent ON protrusion (and therefore ACP pneumatization).

Despite advances in the ability of HRCT to accurately identify dehiscence, distinguishing extremely thin and dehiscent bone remains difficult. Often dehiscence may be suspected on one, or even two, planes of imaging and then bony coverage is clearly shown on an additional view (►**Fig. 9**). In addition, intraoperatively, there may be "clinical dehiscence" where inadequate bony protection is present during probing despite suspected thin bony coverage on CT, further confounding this concept. Until the accuracy of HRCT for clinical dehiscence is known, cases of both extremely

thinned bone and bony dehiscence should be identified to help avoid potential catastrophic complication.

Careful manipulation is required when bony dehiscence of the ICA or ON is present, including when removing the sinus mucosa overlying these structures. Though the risk of injury seems intuitive and is stated in several prior papers, the literature does not provide direct evidence in the form of increasing complication rates for these patients.

Variations due to Existing Pathology or Prior Surgery

The most extensive variability arises from the presence of existing pathology or prior surgical manipulation. The majority of patients in our study had pituitary adenomas, which when large, most often expand the sphenoid sinus, and can demonstrate ICA encasement, cavernous sinus, or bony invasion. Our study had both benign and malignant pathologies ranging from Rathke's cleft cysts to osteosarcoma. Therefore, each case had to be evaluated on a case-by-case basis. Features, such as cavernous sinus invasion by pituitary adenomas (Knosp's classification) are important, though not adequately characterized on the precontrast examinations used in our study.[52]

A small minority of patients in our study had extensive sphenoid invasion by mass. More often patients had destruction of the bone overlying the ICA or ON ("dehiscence by mass"), present in 17 and 5% of patients, respectively, with ICA dehiscence occurring more commonly due to proximity of sellar tumors. This is important to note, because not only is there loss of bony neurovascular protection, there is also loss/distortion of normal anatomic landmarks.

Based on the findings gleaned from the current analysis and previous literature, a preoperative CT checklist is proposed to safely traverse the sphenoid sinuses during sellar and parasellar surgery.

Preoperative CT Checklist

1. Sphenoid sinus pneumatization pattern.
2. Presence of anterior clinoid process and/or dorsum sella pneumatization.
3. Presence of sphenoethmoid cells (Onodi cells).
4. Sphenoid osteology (i.e., small residual sinus, "kissing carotids").
5. Intersphenoid septa and insertion on neurovascular structures (especially with protrusion/extreme bony thinning).
6. Presence of ICA/ON protrusion $\geq$50% or dehiscence.
7. Variations due to existing pathology or prior surgery.

Modeling after the review by O'Brien et al, we attempted to pair this CT checklist with a mnemonic, "SPHENOID," to help clinicians learn this search pattern.[53]

- **S**eptation pattern and septal insertions.
- **P**neumatization pattern (Güldner's classification).
- **H**istory of prior surgery.
- **E**xisting pathology.
- **N**eurovascular protrusion/dehiscence.
- **O**nodi cells.
- **I**ntercarotid distance.
- **D**imensions (sphenoid cavity).

Limitations and Future Directions

The retrospective design did not allow us to assess the accuracy of our dehiscence rates. Defining dehiscence on CT is subject to inter- and intraobserver due to the difficulty of resolving extremely thin bone. Having consistent definitions of anatomic variants should help to limit interobserver variability in future studies. Our sample size was relatively small, though the incidences of anatomic variants were within the range of prior studies. Future evaluation is necessary with prospective studies to evaluate for the accuracy of CT to predict clinical dehiscence and its impact in surgical complications.

Conclusion

Anatomical variations of the sphenoid sinus can impact ease of surgery and potential risk for intraoperative injury to neurovascular structures during transsphenoidal surgery. Our study highlights and reviews the key variants that have potential to impact surgical complications and outcomes in a heterogeneous patient population. The proposed preoperative CT checklist for patients undergoing transsphenoidal surgery consistently identifies these higher risk anatomical variants.

Conflict of Interest
None.

References

1 Ciric I, Ragin A, Baumgartner C, Pierce D. Complications of transsphenoidal surgery: results of a national survey, review of the literature, and personal experience. Neurosurgery 1997;40 (02):225–236, discussion 236–237
2 García-Garrigós E, Arenas-Jiménez JJ, Monjas-Cánovas I, et al. Transsphenoidal approach in endoscopic endonasal surgery for skull base lesions: What radiologists and surgeons need to know. Radiographics 2015;35(04):1170–1185
3 Hammer G, Radberg C. The sphenoidal sinus. An anatomical and roentgenologic study with reference to transsphenoid hypophysectomy. Acta Radiol 1961;56(06):401–422
4 Güldner C, Pistorius SM, Diogo I, Bien S, Sesterhenn A, Werner JA. Analysis of pneumatization and neurovascular structures of the sphenoid sinus using cone-beam tomography (CBT). Acta Radiol 2012;53(02):214–219
5 Hamberger CA, Hammer G, Norlen G, Sjogren B. Transantrosphenoidal hypophysectomy. Arch Otolaryngol 1961;74:2–8
6 Renn WH, Rhoton AL Jr. Microsurgical anatomy of the sellar region. J Neurosurg 1975;43(03):288–298
7 Fujii K, Chambers SM, Rhoton AL Jr. Neurovascular relationships of the sphenoid sinus. A microsurgical study. J Neurosurg 1979;50 (01):31–39
8 Banna M, Olutola PS. Orbital histiocytosis on computed tomography. J Comput Tomogr 1983;7(02):167–170
9 Ouaknine GE, Hardy J. Microsurgical anatomy of the pituitary gland and the sellar region. 2. The bony structures. Am Surg 1987; 53(05):291–297
10 Sethi DS, Pillay PK. Endoscopic management of lesions of the sella turcica. J Laryngol Otol 1995;109(10):956–962
11 Sareen D, Agarwal AK, Kaul JM, Sethi A. Study of sphenoid sinus anatomy in relation to endoscopic surgery. Int J Morphol 2005;23 (03):261–266
12 Abuzayed B, Tanriöver N, Ozlen F, et al. Endoscopic endonasal transsphenoidal approach to the sellar region: results of endoscopic dissection on 30 cadavers. Turk Neurosurg 2009;19(03):237–244

13 Lazaridis N, Natsis K, Koebke J, Themelis C. Nasal, sellar, and sphenoid sinus measurements in relation to pituitary surgery. Clin Anat 2010;23(06):629–636
14 Wang J, Bidari S, Inoue K, Yang H, Rhoton A Jr. Extensions of the sphenoid sinus: a new classification. Neurosurgery 2010;66(04): 797–816
15 Lu Y, Pan J, Qi S, Shi J, Zhang X, Wu K. Pneumatization of the sphenoid sinus in Chinese: the differences from Caucasian and its application in the extended transsphenoidal approach. J Anat 2011;219(02):132–142
16 Perondi GE, Isolan GR, de Aguiar PH, Stefani MA, Falcetta EF. Endoscopic anatomy of sellar region. Pituitary 2013;16(02):251–259
17 Vaezi A, Cardenas E, Pinheiro-Neto C, et al. Classification of sphenoid sinus pneumatization: relevance for endoscopic skull base surgery. Laryngoscope 2015;125(03):577–581
18 Anusha B, Baharudin A, Philip R, Harvinder S, Shaffie BM. Anatomical variations of the sphenoid sinus and its adjacent structures: a review of existing literature. Surg Radiol Anat 2014;36(05):419–427
19 Locatelli M, Di Cristofori A, Draghi R, et al. Is complex sphenoidal sinus anatomy a contraindication to a transsphenoidal approach for resection of sellar lesions? Case series and review of the literature. World Neurosurg 2017;100:173–179
20 Liao JC, Hu GH, Lu YC. Development of the sphenoid sinus affects the surgical approach via saddle area. Acad J Sec Mil Med Univ 2001;22:750–751
21 Kayalioglu G, Erturk M, Varol T. Variations in sphenoid sinus anatomy with special emphasis on pneumatization and endoscopic anatomic distances. Neurosciences (Riyadh) 2005;10(01):79–84
22 Zhou LY. Pneumatic classification of sphenoid sinus and its clinical application. Chin J Anat 2005;28:598–599
23 Hamid O, El Fiky L, Hassan O, Kotb A, El Fiky S. Anatomic variations of the sphenoid sinus and their impact on trans-sphenoid pituitary surgery. Skull Base 2008;18(01):9–15
24 Cho JH, Kim JK, Lee JG, Yoon JH. Sphenoid sinus pneumatization and its relation to bulging of surrounding neurovascular structures. Ann Otol Rhinol Laryngol 2010;119(09):646–650
25 Li SL, Wang ZC, Xian JF. [Study of variations in adult sphenoid sinus by multislice spiral computed tomography]. Zhonghua Yi Xue Za Zhi 2010;90(31):2172–2176
26 Tomovic S, Esmaeili A, Chan NJ, et al. High-resolution computed tomography analysis of variations of the sphenoid sinus. J Neurol Surg B Skull Base 2013;74(02):82–90
27 Wiebracht ND, Zimmer LA. Complex anatomy of the sphenoid sinus: a radiographic study and literature review. J Neurol Surg B Skull Base 2014;75(06):378–382
28 Halawi AM, Simon PE, Lidder AK, Chandra RK. The relationship of the natural sphenoid ostium to the skull base. Laryngoscope 2015;125(01):75–79
29 Rahmati A, Ghafari R, AnjomShoa M. Normal variations of sphenoid sinus and the adjacent structures detected in cone beam computed tomography. J Dent (Shiraz) 2016;17(01):32–37
30 Meloni F, Mini R, Rovasio S, Stomeo F, Teatini GP. Anatomic variations of surgical importance in ethmoid labyrinth and sphenoid sinus. A study of radiological anatomy. Surg Radiol Anat 1992;14(01):65–70
31 Dessi P, Moulin G, Castro F, Chagnaud C, Cannoni M. Protrusion of the optic nerve into the ethmoid and sphenoid sinus: prospective study of 150 CT studies. Neuroradiology 1994;36(07):515–516
32 DeLano MC, Fun FY, Zinreich SJ. Relationship of the optic nerve to the posterior paranasal sinuses: a CT anatomic study. AJNR Am J Neuroradiol 1996;17(04):669–675
33 Sirikci A, Bayazit YA, Bayram M, Mumbuç S, Güngör K, Kanlikama M. Variations of sphenoid and related structures. Eur Radiol 2000; 10(05):844–848
34 Sapçi T, Derin E, Almaç S, Cumali R, Saydam B, Karavuş M. The relationship between the sphenoid and the posterior ethmoid sinuses and the optic nerves in Turkish patients. Rhinology 2004;42(01):30–34
35 Kazkayasi M, Karadeniz Y, Arikan OK. Anatomic variations of the sphenoid sinus on computed tomography. Rhinology 2005;43 (02):109–114
36 Unal B, Bademci G, Bilgili YK, Batay F, Avci E. Risky anatomic variations of sphenoid sinus for surgery. Surg Radiol Anat 2006;28 (02):195–201
37 Hewaidi G, Omami G. Anatomic variation of sphenoid sinus and related structures in Libyan population: CT scan study. Libyan J Med 2008;3(03):128–133
38 Davoodi M, Saki N, Saki G, Rahim F. Anatomical variations of neurovascular structures adjacent sphenoid sinus by using CT scan. Pak J Biol Sci 2009;12(06):522–525
39 Batra PS, Citardi MJ, Gallivan RP, Roh H-J, Lanza DC. Software-enabled CT analysis of optic nerve position and paranasal sinus pneumatization patterns. Otolaryngol Head Neck Surg 2004;131 (06):940–945
40 Itagi RM, Adiga CP, Kalenahalli K, Goolahally L, Gyanchandani M. Optic nerve canal relation to posterior paranasal sinuses in Indian ethnics: Review and objective classification. J Clin Diagn Res 2017;11(04):TC01–TC03
41 Dal Secchi MM, Dolci RLL, Teixeira R, Lazarini PR. An analysis of anatomic variations of the sphenoid sinus and its relationship to the internal carotid artery. Int Arch Otorhinolaryngol 2018;22 (02):161–166
42 Szolar D, Preidler K, Ranner G, et al. The sphenoid sinus during childhood: establishment of normal developmental standards by MRI. Surg Radiol Anat 1994;16(02):193–198
43 Tan HK, Ong YK. Sphenoid sinus: an anatomic and endoscopic study in Asian cadavers. Clin Anat 2007;20(07):745–750
44 United States Census Bureau. Annual social and economic (ASEC) supplement of the current population survey (CPS Available at: https://www.census.gov/programs-surveys/saipe/guidance/model-input-data/cpsasec.html. Accessed May 06, 2019
45 da Costa MDS, de Oliveira Santos BF, de Araujo Paz D, et al. Anatomical variations of the anterior clinoid process: a study of 597 skull base computerized tomography scans. Oper Neurosurg (Hagerstown) 2016;12(03):289–297
46 Arslan H, Aydinlioğlu A, Bozkurt M, Egeli E. Anatomic variations of the paranasal sinuses: CT examination for endoscopic sinus surgery. Auris Nasus Larynx 1999;26(01):39–48
47 Burulday V, Muluk NB, Akgül MH, Kaya A, Öğden M. Presence and types of anterior clinoid process pneumatization, evaluated by multidetector computerized tomography. Clin Invest Med 2016; 39(03):E105–E110
48 Isyk AO, Bulut S. Concha bullosa: relations with sinus disease and septal deviation. Turk J Diagn Intervent Radiol 1994;1:301–304
49 Driben JS, Bolger WE, Robles HA, Cable B, Zinreich SJ. The reliability of computerized tomographic detection of the Onodi (Sphenoethmoid) cell. Am J Rhinol 1998;12(02):105–111
50 Chatrath P, Nouraei SA, De Cordova J, Patel M, Saleh HA. Endonasal endoscopic approach to the petrous apex: an image-guided quantitative anatomical study. Clin Otolaryngol 2007;32(04):255–260
51 Standring S. Gray's Anatomy: The Anatomical Basis of Clinical Practice. 41st ed. Philadelphia, PA: Elsevier; 2015:556–570
52 Micko AS, Wöhrer A, Wolfsberger S, Knosp E. Invasion of the cavernous sinus space in pituitary adenomas: endoscopic verification and its correlation with an MRI-based classification. J Neurosurg 2015;122(04):803–811
53 O'Brien WT Sr, Hamelin S, Weitzel EK. The preoperative sinus CT: Avoiding a "CLOSE" call with surgical complications. Radiology 2016;281(01):10–21